Semiconductors

Photonic Crystals with Thermally Switchable Stop Bands Fabricated from Se@Ag_2Se Spherical Colloids**

*Unyong Jeong and Younan Xia**

Self-assembly of monodispersed spherical colloids into highly ordered lattices has attracted considerable attention due to the potential use of these periodic structures as photonic crystals.[1] Despite intensive study on this subject, the building blocks available to form long-range ordered lattices have been mainly limited to polymer latexes and silica beads.[2] To obtain wider photonic band gaps by increasing the contrast in refractive index, processing materials with refractive indices greater than 2 into monodispersed spherical colloids is of the utmost necessity.[3] Although a number of semiconductors (e.g., ZnS, CdS, and TiO_2) with relatively high refractive indices have been recently synthesized as monodispersed spheres and then crystallized into 3D opaline lattices with strong stop bands in the visible region,[4] the diversity of materials still needs to be greatly expanded to fully capitalize on the advantages and exploit the potential brought by the large contrast in refractive index. Very recently, we developed a solution-phase method for the large-scale production of monodispersed amorphous selenium (*a*-Se) spherical colloids with readily controllable sizes.[5] Herein we demonstrate that the high reactivity of Se towards Ag atoms could be used to generate monodispersed spherical colloids consisting of *a*-Se cores and Ag_2Se shells. More interestingly, the reversible phase transition associated with Ag_2Se provides a new platform for fabricating photonic crystals with thermally switchable stop bands.

As a semiconductor with a narrow band gap, Ag_2Se has a range of interesting and useful properties. It undergoes a phase transition at 133 °C with a remarkable change in the electronic property.[6] The low-temperature β-phase crystallizes in an orthorhombic lattice and acts as a semiconductor. It is a good candidate for thermoelectric applications due to its low lattice thermal conductivity ($\approx 5\ mW\,cm^{-1}\,K$), high electrical conductivity ($\approx 2000\ S\,cm^{-1}$), and hence a relatively large Seebeck coefficient (about $-150\ \mu V\,K^{-1}$).[7] It was also demonstrated that slight changes in stoichiometry to $Ag_{2+\delta}Se$ (in the same orthorhombic lattice) can induce appreciable magnetoresistance.[8] An explanation to account for this property considers the existence of small silver clusters in the crystal lattice.[9] Nonstoichiometric solids have also been reported to exist in tetragonal, face-centered cubic (fcc), monoclinic, or triclinic structures at room temperature.[10] Recently, Alivisatos and co-workers reported the use of a cation-exchange reaction to transform Ag_2Se nanocrystals into CdSe without causing any change to the morphology.[11] The high-temperature phase, α-Ag_2Se, has a body-centered cubic (bcc) structure and is a good superionic conductor as a result of the high mobility of silver cations and the low activation energy for diffusion and conduction.[12] The polymorphic transition between the β- and α-phases has been shown to be reversible.

We note that photonic crystals with tunable stop bands have been exploited as sensors to detect and monitor the variation in temperature, strain, and concentration of a chemical or biochemical species.[13–16] Recently, our group also demonstrated color writing and printing by embedding photonic crystals in elastomeric matrices.[17] The essence of this research is to take advantage of the reversible, polymorphic transition of a solid material to fabricate photonic crystals with stop bands that can be reversibly switched between two spectral positions. Such a system can potentially serve as an optical switch or a thermally printable medium.

It has been demonstrated that β-Ag_2Se nanowires could be produced by reacting nanowires of trigonal selenium (*t*-Se, serving as a chemical template) with $AgNO_3$ in an aqueous solution at room temperature [Eq. (1)].[18] In this particular

$$3\,Se_{(s)} + 6\,Ag^{+}_{(aq)} + 3\,H_2O \rightarrow 2\,Ag_2Se_{(s)} + Ag_2SeO_{3(s)} + 6\,H^{+}_{(aq)} \quad (1)$$

route, the formation of monoclinic Ag_2SeO_3 as a by-product was inevitable.

Herein we wish to report a new process, in which $AgNO_3$ is reduced by ethylene glycol to generate Ag atoms that further react with spherical colloids of *a*-Se to form monodispersed colloids consisting of *a*-Se cores and β-Ag_2Se shells. The *a*-Se colloids with smooth surfaces and controllable sizes are, in turn, synthesized by using a chemical solution-phase method based on the reduction of selenious acid with excessive hydrazine in ethylene glycol.[5] After residual hydrazine has been removed, $AgNO_3$ dissolved in ethylene glycol is added to generate *a*-Se@Ag_2Se core–shell colloids.

[*] Dr. U. Jeong, Prof. Y. Xia
Department of Chemistry, University of Washington
Seattle, WA 98195-1700 (USA)
Fax: (+1) 206-685-8665
E-mail: xia@chem.washington.edu

[**] This work was supported in part by the STC Program of the National Science Foundation (NSF) under Agreement Number DMR-0120967 and a Fellowship from the David and Lucile Packard Foundation. Y.X. is an Alfred P. Sloan Fellow (2000) and a Camille Dreyfus Teacher Scholar (2002). U.J. has also received partial support from the Post-Doctoral Fellowship Program of the Korean Science and Engineering Foundation (KOSEF).

Supporting information for this article is available on the WWW under http://www.angewandte.org or from the author.

 DOI: 10.1002/ange.200462906

The extent of conversion from *a*-Se to Ag_2Se can be controlled by adjusting the molar ratio of $AgNO_3$ to *a*-Se.

The formation of Ag_2Se was first confirmed by powder X-ray diffraction (XRD, Philips PW-1710 diffractometer). As shown in Figure 1 A, the as-synthesized colloids of *a*-Se

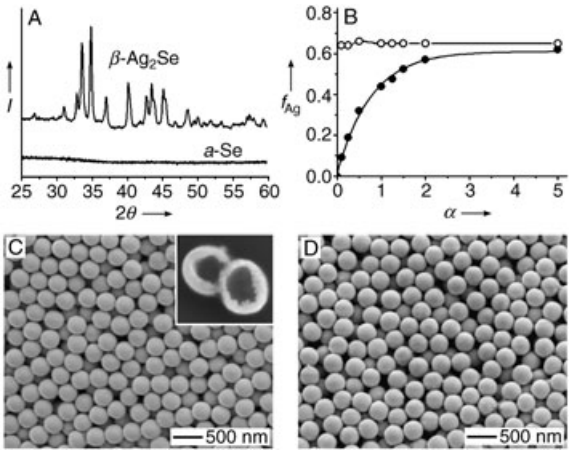

Figure 1. A) XRD patterns taken from the as-synthesized *a*-Se and *a*-Se@Ag_2Se colloids (with $f_{Ag} = 0.32$). All peaks were indexed to orthorhombic β-Ag_2Se. B) Plots showing how f_{Ag} of the core–shell colloids changed as the molar ratio (α) of $AgNO_3$ to Se varied. Solid circles and open circles represent f_{Ag} values measured by using EDX before and after removal of the Se cores with hydrazine, respectively. C) SEM image of core–shell colloids synthesized with $\alpha = 0.5$. The inset shows a SEM image of two broken colloids after the *a*-Se cores had been dissolved with hydrazine. D) SEM image of another batch of core–shell colloids synthesized with $\alpha = 2.0$.

displayed no diffraction peak in the entire 2θ range from 25 to 60°, which indicates an amorphous structure. The XRD pattern taken from the product (synthesized with a molar ratio of 0.5 $AgNO_3$ to 1.0 Se) matched the orthorhombic lattice of β-Ag_2Se (lattice constants: $a = 4.33$, $b = 7.06$, $c = 7.76$ Å). The XRD patterns were essentially the same regardless of the ratio of $AgNO_3$ to Se involved in the synthesis. It is worth mentioning that no impurity such as Ag_2SeO_3 was detected in the as-synthesized product; this lack of impurity is because ethylene glycol was able to reduce Ag^+ cations to Ag atoms, which then diffused quickly into the lattice of *a*-Se to generate β-Ag_2Se as the sole product [Eq. (2)].

$$2\,Ag + Se \rightarrow Ag_2Se \qquad (2)$$

For the as-obtained core–shell colloids, we used energy-dispersive X-ray spectra (EDX, Genesis 2000, EDAX Inc., Mahwah, NJ) to determine the elemental composition, or the atomic fraction of silver (f_{Ag}). To improve the signal-to-noise ratio and thus obtain reliable data, we used a thick slab (≈ 6 μm) of the colloid sample deposited on a silicon wafer in combination with a beam spot of > 100 μm^2. EDX peaks that corresponded to the L shell of Ag and Se were employed for all quantitative analyses. Figure 1 B shows the change in f_{Ag} (solid circles) with increasing molar ratio of $AgNO_3$ to Se ($\alpha = [AgNO_3]/[Se]$) and demonstrates a monotonic increase as α changed from 0 to 5. To determine the atomic fraction of Ag in the shells only, the Se cores were selectively removed by immersing the sample in hydrazine for 18 h. As the Ag_2Se shells were polycrystalline, the Se cores were slowly etched away by hydrazine through the grain boundaries. The atomic fractions of Ag for the etched samples are presented as open circles in Figure 1 B; essentially the same value ($\approx 65\%$) was obtained regardless of the α value. This percentage matches the stoichiometry of Ag_2Se, which indicates that the Ag_2Se shells were very pure. The plots also show that the *a*-Se colloids can only be completely converted into Ag_2Se when the molar ratio of $AgNO_3$ to Se is higher than 5.

Figure 1 C and D show scanning electron microscopy (SEM, Siron XL, FEI, Hillsboro, OR) images of two typical samples obtained at different molar ratios of $AgNO_3$ to Se: 0.5:1 and 2:1. As with the *a*-Se colloids, the core–shell particles were spherical, monodispersed, and had featureless surfaces. The inset in Figure 1 C gives a SEM image of the same sample after the unconverted *a*-Se cores had been selectively removed by extraction with hydrazine. On the basis of both SEM and XRD results, we concluded that the as-obtained products were composed of Se cores (amorphous) and β-Ag_2Se shells (polycrystalline). Once the f_{Ag} value of a sample had been determined by EDX, both the shell thickness and the dimensional change involved in this template-engaged reaction was estimated. For instance, the calculated diameter and shell thickness of the colloids displayed in Figure 1 C are 310 and 22 nm, respectively, which are in good agreement with the results from TEM studies. The derivation of these values is provided as Supporting Information, together with experimental results.

Both Se and Ag_2Se transform into different phases as the temperature is raised from room temperature to about 150 °C: Se undergoes a transition from amorphous to trigonal phase at 31 °C whereas Ag_2Se has a phase transition (from β to α) around 133 °C. We have followed the phase transitions of both cores and shells with XRD. In a typical experiment, a thick film (≈ 1 mm) was cast on a glass slide from an aqueous suspension of core–shell colloids and dried in air. The sample was annealed at various temperatures ranging from room temperature to 150 °C with increasing steps of ≈ 10 °C. The sample was annealed at each set temperature for 10 min and then quenched by placing it on a cold metal plate. XRD measurements were taken immediately after quenching and were completed within 10 min. Figure 2 shows XRD patterns taken from the same sample as that given in Figure 1 D ($f_{Ag} = 0.56$). The diffraction pattern at room temperature was similar to that shown in Figure 1 A, although different values of f_{Ag} were involved. After the sample had been annealed at 110 °C, a small new peak (indicated by the asterisk in Figure 2) appeared at $2\theta = 28.5°$, which corresponds to the (101) diffraction of *t*-Se. After the sample had been annealed at 150 °C, the peaks associated with β-Ag_2Se mostly disappeared and a characteristic peak of α-Ag_2Se (with a bcc structure) appeared at $2\theta = 35.2°$ (indicated by the triangular in Figure 2); this peak was indexed to the (200) diffraction. The sample reverted to the β-Ag_2Se structure when it was cooled slowly to 110 °C. It is worth pointing out that the peak from *t*-Se remained the same in the β↔α transition for the

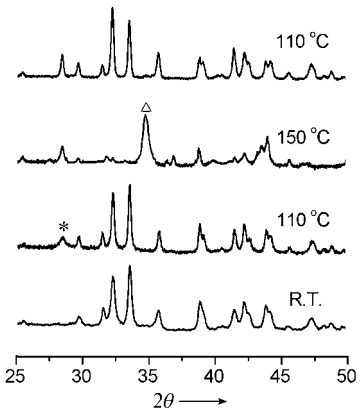

Figure 2. XRD patterns taken from a sample of Se@Ag_2Se core–shell colloids at room temperature, which were then heated to 110 and 150 °C, followed by cooling to 110 °C. The sample was annealed at each temperature for 10 min and quenched on a cold metal plate and XRD measurement was taken within 10 min. ⋆ and △ represent the peaks for *t*-Se and α-Ag_2Se, respectively.

Ag_2Se shells. These results indicate that the Se core was well preserved inside the Ag_2Se shell as the sample underwent thermal annealing. The XRD results confirm that the phase transition between orthorhombic and bcc structure for the Ag_2Se shells is reversible. SEM studies also showed that the spherical shape of these core–shell colloids was maintained through multiple cycles of such phase transitions when $f_{Ag} = 0.56$. In comparison, the shells with $f_{Ag} = 0.32$ were broken in the annealing process and the Se leaked from the shells and aggregated into large, irregular structures.

The thermally reversible transition between two different states for the Ag_2Se shells implies that these core–shell colloids could be used as building blocks to fabricate photonic crystals with reversibly switchable stop bands. To this end, we have crystallized core–shell colloids ($f_{Ag} = 0.56$) into 3D opaline lattices on glass substrates by using a previously reported method.[19] Figure 3 shows the cross-sectional SEM images of a typical sample, which displays an fcc structure with its {111} planes oriented parallel to the surface of the supporting substrate. Figure 3 A shows an image of the as-obtained sample, and Figure 3 B shows the same sample after it had been annealed at 150 °C for 10 min, then quenched to room temperature by placing it on a cold metal plate. Even though the core–shell colloids went through two phase transitions from *a*-Se to *t*-Se and from β-Ag_2Se to α-Ag_2Se, the spherical shape of the colloids and the long-range order of the lattice were both essentially retained. As long as the Se cores did not leak out (or if they were removed in advance), the phase transition between β- and α-Ag_2Se could go through many cycles of heating and cooling without causing significant changes to the opaline lattices.

Figure 4 shows the near-IR reflection spectra taken from an opaline lattice assembled from core–shell colloids with $f_{Ag} = 0.56$. The spectra were recorded by using a fiber-optic spectrometer (NIR-128, Control Development, South Bend, IN) with an incident and detection angle of 10° from the normal to the surface. The opaline lattice was annealed at various temperatures up to 150 °C with a step increase of

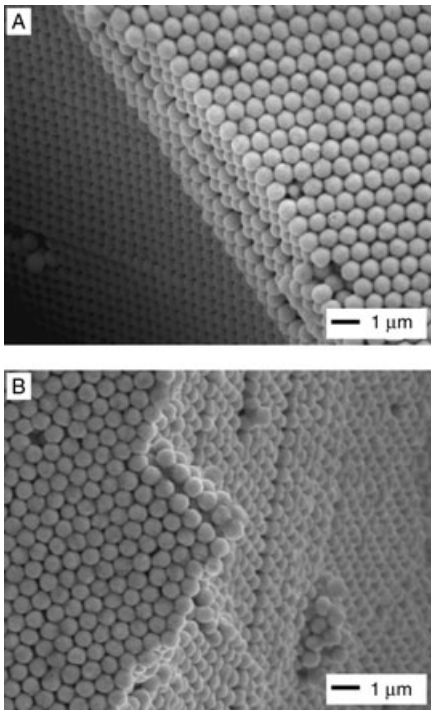

Figure 3. A) Cross-sectional SEM image of an opaline lattice assembled from *a*-Se@Ag_2Se colloids with $f_{Ag} = 0.56$. B) The same sample, after it had been annealed at 150 °C for 10 min.

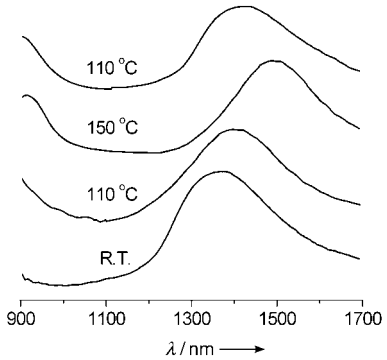

Figure 4. Reflection spectra in the near-IR region taken from an opaline lattice consisting of Se@Ag_2Se core–shell colloids with $f_{Ag} = 0.56$. The temperature was increased from room temperature to 110 and 150 °C, and then reduced to 110 °C. After the sample had been annealed at each temperature for 10 min, it was quenched to preserve the high-temperature phases.

10 °C. After annealing for 10 min at each temperature, the sample was quenched (by placing it on a cold metal plate) to preserve the high-temperature phases. We did not observe any significant change in the peak position until 70 °C. When the annealing temperature was increased to 80 °C, the peak suddenly red-shifted to 1392 nm and then showed little change as the temperature was further raised to 130 °C. This change was attributed to the increase in the refractive index when the cores were converted from *a*-Se into *t*-Se. In the range of 130–140 °C, the peak was red-shifted again to 1497 nm as the Ag_2Se shells underwent a transition from

the β- to the α-phase. The peak shifted back to 1415 nm when the sample was annealed at 110 °C, and then quenched to room temperature.

The observed reflectance peaks and shifts can be explained on the basis of the Bragg diffraction equation. The refractive index of β-Ag_2Se was obtained by plotting the data reported for the UV/Vis region[20] and fitting them with the first-order Sellmeier equation (Eq. (3)),[21] in which $A =$

$$n^2(\lambda) = A + B[\lambda^2/(\lambda^2 - C)] \quad (3)$$

5.20, $B = 3.62$, and $C = 0.13$; and the unit for λ is μm. From this equation, the refractive index of β-Ag_2Se was calculated as 2.98 at $\lambda = 2$ μm. The Moss relationship, $n^4 E_g = 95$,[22] could not be applied to this system as the value of the band gap (E_g) of β-Ag_2Se is still being disputed. The reported values, −0.17,[23] 1.33,[24] 1.58,[25] and 2.17 eV,[26] would suggest very different refractive indices: 4.86, 2.90, 2.88, and 2.44, respectively. The volume fraction of the shell and the core were calculated (see the Supporting Information). For core–shell colloids with $f_{Ag} = 0.56$, the volume fraction of the core (X_{core}) was 23 %. The dielectric constant of the core–shell colloids was calculated by assuming a linear relationship between the dielectric constant and the volume fraction [Eq. (4)].[27] With

$$n = n_{core} X_{core} + n_{shell}(1 - X_{core}) \quad (4)$$

the reported refractive index of 2.45 for *a*-Se,[28] a value of 2.86 was obtained for the refractive index of core–shell colloids with $f_{Ag} = 0.56$.

Based on the assumption of a closely packed structure (26 % air), the reflectance peak centered at ≈1365 nm for the sample annealed at room temperature was assigned to the diffraction from (111) lattice planes. From the Bragg diffraction equation,[29] the peak position was calculated as 1358 nm with a refractive index of 2.86 for the core–shell colloids. The higher refractive index of *t*-Se (2.8 at 2 μm versus 2.45 for *a*-Se)[30] increased the refractive index of the core–shell particles to 2.94. This increase in refractive index led to a red shift for the (111) peak to ≈1395 nm, which matched the experimental result. After the sample had been annealed at 150 °C, the (111) diffraction peak was further shifted to ≈1497 nm and a new peak appeared at ≈919 nm. The red shift was induced by the phase transition from β- to α-Ag_2Se, that is, from a semiconductor to a superionic state. From the peak position of the (111) plane, the refractive index of α-Ag_2Se was estimated to be 3.26. This refractive index could be used to assign the peak at ≈919 nm as the diffraction from (220) lattice planes (calculation: 916 nm). The Moss relationship[22] predicted a band-gap energy of 0.84 eV for α-Ag_2Se, which is much lower than that of β-Ag_2Se obtained from our refractive index value (1.20 eV). Note that the band gap of α-Ag_2Se is still in the range of semiconductors. The increase in conductivity accompanying the transition from the β- to the α-phase mainly results from the enhanced mobility of the Ag cations. When the sample was cooled down to 110 °C, the diffraction peaks were recovered with some slight thermal hysteresis: 1415 nm for the (111) diffraction and below 900 nm for the (220) diffraction. The peaks did not shift anymore when the sample was annealed again at temperatures below 110 °C, which suggests that the phase transition between *a*-Se and *t*-Se was irreversible.

This study focuses on how thermally induced polymorphic transitions can lead to changes in the photonic band gap. Photonic crystals with a band gap in the visible region can serve as photonic papers, which is one of the primary uses for core–shell colloids. For example, a phase transition of the photonic crystals can be induced in a confined region with the aid of a laser and subsequent quenching to room temperature can preserve the kinetically trapped patterns. These altered regions will diffract light of longer wavelengths than will do other regions, thus enabling colored patterns to be recorded. If the photonic crystals are annealed at an elevated temperature, the patterns can be readily erased. In addition, the electrical conductivity of β-Ag_2Se ($\approx 2000\ S\,cm^{-1}$) is exceptionally high relative to those of other semiconductors.[7] This value can be further increased to $\approx 6000\ S\,cm^{-1}$ in the α-Ag_2Se phase.[7c] These unique properties will make the *a*-Se@Ag_2Se core–shell colloids potentially useful in thermoelectric applications.

In summary, we have exploited the high reactivity of *a*-Se towards Ag atoms to produce core–shell spherical colloids in the form of *a*-Se@Ag_2Se. Upon heating, the cores and shells change phase from *a*-Se to *t*-Se and from β-Ag_2Se to α-Ag_2Se, respectively. When the shells were sufficiently thick (55 nm, or with $f_{Ag} = 0.56$), the core–shell colloids maintained their spherical shape while undergoing multiple cycles of phase transitions between β-Ag_2Se and α-Ag_2Se. This feature has been used to fabricate photonic crystals with thermally switchable stop bands.

Experimental Section

In a typical synthesis, hydrazine hydrate (55 % N_2H_4; Aldrich) in ethylene glycol (0.35 M, 80 mL) was added to pure ethylene glycol (400 mL; J. T. Baker) in a 1000-mL Erlenmeyer flask. After the mixture had been stirred for 10 min, H_2SeO_3 (Aldrich, 99.99 %) in ethylene glycol (0.07 M, 80 mL) was introduced and the reaction was allowed to proceed for 2 h. As hydrazine can also reduce $AgNO_3$ to Ag nanoparticles and agglomerates, all remaining hydrazine in the suspension of *a*-Se colloids was removed by vacuum distillation before $AgNO_3$ was added to the reaction system. To form Ag_2Se, a solution of poly(vinylpyrrolidone) (PVP; 15 mL, $\bar{M}_w = 55\,000$, 3 g per 200 mL; Aldrich) in ethylene glycol was added at room temperature to the *a*-Se that had been suspended in ethylene glycol (30 mL). Adding a solution of $AgNO_3$ (Aldrich, 99.9 %) in ethylene glycol to this suspension resulted in a change from red to dark brown then dark blue as the ratio between $AgNO_3$ and *a*-Se increased. The reaction mixture was diluted with water (100 mL) and the core–shell colloids were collected by centrifugation. To remove ethylene glycol and excess PVP, the product was again diluted with water (100 mL) and separated by centrifugation. This washing cycle was repeated several times before the product was dried in air. The colloids were stable in air and did not aggregate.

Received: December 11, 2004
Published online: April 12, 2005

Keywords: colloids · selenium · semiconductors · silver

[1] See, for example: a) C. López, *Adv. Mater.* **2003**, *15*, 1679; b) special issue "Materials Science Aspects of Photonic Crystals": A. Polman, P. Wiltzius, *MRS Bull.* **2001**, *26*, 608; c) special issue "Photonic Crystals": Y. Xia, *Adv. Mater.* **2001**, *13*, 369; d) O. D. Velev, A. M. Lenhoff, *Curr. Opin. Colloid Interface Sci.* **2000**, *5*, 56; e) A. Stein, R. C. Schroden, *Curr. Opin. Solid State Mater. Sci.* **2001**, *5*, 553; f) Y. A. Vlasov, X. Z. Bo, J. C. Sturm, D. J. Norris, *Nature* **2001**, *414*, 289; g) J. F. Bertone, P. Jiang, K. S. Hwang, D. M. Mittleman, V. L. Colvin, *Phys. Rev. Lett.* **1999**, *83*, 300; h) D. Wang, R. A. Caruso, F. Caruso, *Chem. Mater.* **2001**, *13*, 364; i) W. M. Lee, S. A. Prunziski, P. V. Braun, *Adv. Mater.* **2002**, *14*, 271.

[2] a) R. Arshady, *Colloid Polym. Sci.* **1992**, *270*, 717; b) W. Stöber, A. Fink, E. Bohn, *J. Colloid Interface Sci.* **1968**, *26*, 62.

[3] J. D. Joannopoulos, R. D. Meade, J. N. Winn, *Photonic Crystals*, Princeton University, Princeton, **1995**.

[4] a) E. Matijević, D. Murphy-Wilhelmy, *J. Colloid Interface Sci.* **1982**, *86*, 476; b) D. Murphy-Wilhelmy, E. Matijević, *J. Chem. Soc. Faraday Trans.* **1984**, *80*, 563; c) K. P. Velikov, A. van Blaaderen, *Langmuir* **2001**, *17*, 4779; d) M. L. Breen, A. D. Dinsmore, R. H. Pink, S. B. Qadri, B. R. Ratna, *Langmuir* **2001**, *17*, 903; e) X. Jiang, T. Herricks, Y. Xia, *Adv. Mater.* **2003**, *15*, 1205.

[5] U. Jeong, Y. Xia, *Adv. Mater.* **2005**, *17*, 102.

[6] a) Y. Kumashiro, T. Ohachi, I. Taniguchi, *Solid State Ionics* **1996**, *86*, 761; b) M. C. Santhosh Kumar, B. Pradeep, *Bull. Mater. Sci.* **2002**, *25*, 407.

[7] a) M. Ferhat, J. Nagao, *J. Appl. Phys.* **2000**, *88*, 813; b) V. Damodars Das, D. Karunakaran, *J. Appl. Phys.* **1990**, *67*, 15; c) M. C. S. Kumar, B. Pradeep, *Bull. Mater. Sci.* **2002**, *25*, 407.

[8] a) R. Xu, A. Husmann, T. F. Rosenbaum, M.-L. Saboungi, J. E. Enderby, P. B. Littlewood, *Nature* **1997**, *390*, 57; b) G. Beck, J. Janek, *Phys. B* **2001**, *308*, 1086.

[9] a) A. A. Abrikosov, *Phys. Rev. B* **1998**, *58*, 2788; b) A. A. Abrikosov, *Europhys. Lett.* **2000**, *49*, 789.

[10] a) T. Okabe, K. Ura, *J. Appl. Crystallogr.* **1994**, *27*, 140; b) L. V. Constantinescu, *Thin Solid Films* **1976**, *32*, 333; c) Y. Saito, M. Sato, M. Shiojiri, *Thin Solid Films* **1981**, *79*, 257; d) A. G. Abdullayev, R. B. Shafizade, E. S. Krupnikov, K. V. Kiriluk, *Thin Solid Films* **1983**, *106*, 175.

[11] D. H. Son, S. M. Hughes, Y. Yin, A. P. Alivisatos, *Science* **2004**, *306*, 1009.

[12] a) M. A. Hamilton, A. C. Barnes, W. S. Howells, H. E. Fischer, *J. Phys. Condens. Matter* **2001**, *13*, 2425; b) J. P. Rino, Y. M. Hornos, G. A. Antonio, I. Ebbsjö, R. K. Kalia, P. Vashishta, *J. Chem. Phys.* **1988**, *89*, 7542.

[13] a) J. M. Weissman, H. B. Sunkara, A. S. Tse, S. A. Asher, *Science* **1996**, *274*, 959; b) S. Valkama, H. Kosonen, J. Ruokolainen, T. Haatainen, M. Torkkeli, R. Serimaa, G. T. Brinke, O. Ikkala, *Nat. Mater.* **2004**, *3*, 872; c) Z. B. Hu, X. H. Lu, J. Gao, *Adv. Mater.* **2001**, *13*, 1708; d) J. D. Bebord, S. Eustis, S. B. Debord, M. T. Lofye, L. A. Lyon, *Adv. Mater.* **2002**, *14*, 658.

[14] a) J. H. Holtz, S. A. Asher, *Nature* **1997**, *389*, 829; b) C. E. Reese, M. E. Baltusavich, J. P. Keim, S. A. Asher, *Anal. Chem.* **2001**, *73*, 5038; c) C. F. Blanford, R. C. Schroden, M. Al-Daous, A. Stein, *Adv. Mater.* **2001**, *13*, 26.

[15] a) T. Cassagneau, F. Caruso, *Adv. Mater.* **2002**, *14*, 1629; b) Z.-Z. Gu, R. Horie, S. Kubo, Y. Yamada, A. Fijishima, O. Sato, *Angew. Chem.* **2002**, *114*, 1201; *Angew. Chem. Int. Ed.* **2002**, *41*, 1153.

[16] a) S. H. Foulger, P. Jiang, A. C. Lattam, D. W. Smith, J. Ballato, *Langmuir* **2001**, *17*, 6023; b) K. Sumioka, H. Kayashima, T. Tsutsui, *Adv. Mater.* **2002**, *14*, 1284.

[17] a) H. Fudouzi, Y. Xia, *Adv. Mater.* **2003**, *15*, 892; b) H. Fudouzi, Y. Xia, *Langmuir* **2003**, *19*, 9653.

[18] a) B. Gates, Y. Wu, Y. Yin, P. Yang, Y. Xia, *J. Am. Chem. Soc.* **2001**, *123*, 11500; b) B. Gates, B. Mayers, B. Cattle, Y. Xia, *Adv. Funct. Mater.* **2002**, *12*, 219.

[19] S. H. Park, D. Qin, Y. Xia, *Adv. Mater.* **1998**, *10*, 1028.

[20] V. Hönig, A. Thomas, *Phys. Status Solidi A* **1987**, *100*, K81.

[21] D. T. F. Marple, *J. Appl. Phys.* **1964**, *35*, 539.

[22] T. S. Moss, *Phys. Status Solidi B* **1985**, *131*, 415.

[23] A. G. Abdullayev, R. B. Shafizade, E. S. Kruprikov, K. V. Kiriluk, *Thin Solid Films* **1983**, *106*, 175.

[24] A. B. Kulkarni, M. D. Uplane, C. D. Lokhande, *Thin Solid Films* **1995**, *120*, 14.

[25] M. C. Santhosh Kumar, B. Pradeep, *Semicond. Sci. Technol.* **2002**, *17*, 261.

[26] R. Harpeness, O. Palchik, A. Gedanken, V. Palchik, S. Amiel, M. A. Slifkin, A. M. Weiss, *Chem. Mater.* **2002**, *14*, 2094.

[27] H. Takeda, K. Yoshino, *Appl. Phys. Lett.* **2002**, *80*, 24.

[28] a) P. Nagels, E. Sleeckx, R. Callaerts, E. Márquez, J. M. González, A. M. Bernal-Oliva, *Solid State Commun.* **1997**, *102*, 539; b) T. Innami, T. Miyazaki, A. Adachi, *J. Appl. Phys.* **1999**, *86*, 1382.

[29] a) P. L. Flaugh, S. E. O'Donnell, S. A. Asher, *Appl. Spectrosc.* **1984**, *38*, 847; b) J. Jethmalani, W. Ford, *Chem. Mater.* **1996**, *8*, 2146.

[30] E. D. Palik in *Handbook of Optical Constants of Solid*, *Vol. 2* (Ed.: E. D. Palik), Academic Press, Orlando, **1985**, p. 691.

